AI-Powered Skin Disease Detection Using Adaptive Particle Swarm Intelligent Optimization and Hyper-Convolutional Neural Networks

N Annalakshmi[1], S Umarani[2]*
Research Scholar, Department of Computer Science, SRMIST, Ramapuram, Chennai, Tamil Nadu, India[1]
Professor, Department of Computer Science and Applications (BCA), SRMIST, Ramapuram, Chennai, Tamil Nadu, India[2]

***Abstract*—In recent medical research, skin cancer has emerged as one of the most prevalent and fatal cancers globally. Previous studies have faced challenges in detecting skin cancer early due to the complexity of identifying specific skin diseases, segmenting affected areas, and selecting relevant features. To address these limitations, this study proposes a novel AI-powered enhanced skin disease detection system that applies an Adaptive Particle Swarm Intelligent Optimization (APSIO) in conjunction with a Hyper-Convoluted Intra-Capsuled Neural Network (HCI-CNN). In image processing, a Gaussian Wavelet Spectral Filter is initially used to preprocess the input dataset of skin-cancer images. This filter is used to standardize the skin layer of the pixel. After preprocessing, the method applies Slice Fragment Window Segmentation (SFWS) to divide the image into several clusters, focusing on the specified area affected by the disease. Next, Adaptive Particle Swarm Intelligent Optimization (APSIO) is applied for feature selection. APSIO is an optimization metaheuristic algorithm that optimizes the selection of relevant features from the segmented image. After removing evaluated and non-effective features, YOLO extracted features are passed through an HCI-CNN classifier to efficiently characterize high-level spatial hierarchies and relations of features in the feature space using hyper-convolutional operations and capsule representations. This paper analyzed the clinical images of individuals along with the dataset images. The output gain improved Accuracy to 97%, precision to 96.52%, recall to 96.55%, and F1-score to 96.93%, while simultaneously minimizing false positives and total time complexity.**

***Keywords*—Skin cancer; image preprocessing; hyper-convoluted intra-capsuled neural network (HCI-CNN); adaptive Particle Swarm Intelligent Optimization (APSIO); image classification**

I. Introduction

Early skin cancer detection continues to be challenging because of its aggressive nature and higher mortality rate when it is not treated. The delayed diagnosis of melanoma considerably reduces the survival rate of the patient, allowing the cancer to grow quickly to its terminal phase and spread. Most other skin cancers, including basal cell carcinoma, pose serious health threats due to high prevalence and potential severity. The phrase "Skin condition" describes any condition that tends to affect the skin, which is the biggest organ in the human body and one of many organs that make up the body. Automated classification [1]-[2] assists in reducing dissimilarity among samples, whereas proper skin disease detection is crucial for successful preprocessing and diagnosis. Actinic keratosis, an occasional precursor to squamous cell carcinoma, typically presents as a dry, scaly spot on the skin.

Hereditary conditions may also result in skin disorders. The shallow, thin outer layer of skin. These diseases can lead to physical and psychological damage. Basal cell carcinoma [3] is the most common type of skin cancer that occurs in the outermost layer of the epidermis' basal cells. In addition, the sun-exposed sites often include the hands, neck, ears, and scalp, where squamous cell carcinoma, the second most common skin cancer, arises from epidermal squamous cells.

It can extend and infiltrate into deeper skin layers. In medical image analysis, skin disease classification entails distinguishing and differentiating among different situations based on their image characteristics [4]. This procedure characteristically depends on skin-layer imaging to detect such melanoma, and recent approaches employ machine learning and deep learning to evaluate the accuracy, especially CNN.

The three components of the prediction element, the ensemble model, the predictive aggregator module, and the pre-processing unit. The preprocessing module provides the proper preprocessing, such as scaling, normalization, and image changes, to the images in the dataset. The factors [5] to consider are the mutation amount, which randomly modifies the values of the chromosomes, and the random cross-over rate, which determines the likelihood of a random crossing occurring independent of the fitness parameter.

A. Research Objective

The primary objective of this study is to develop an advanced, AI-driven skin cancer detection system that enhances the accuracy and efficiency of diagnosis by integrating multiple novel techniques. Specifically, the research aims to:

- Reduce the skin blur area and improve the image quality according to skin cancer using a Gaussian Wavelet Spectral Filter.
- Accurately localize diseased regions via Slice Fragment Window Segmentation (SFWS), enabling precise clustering of affected areas.
- Optimize feature selection using Adaptive Particle Swarm Intelligent Optimization (APSIO), thereby

*Corresponding Author

eliminating redundant or irrelevant features to improve classifier performance.

- Enhance classification performance by deploying a Hyper-Convoluted Intra-Capsuled Neural Network (HCI-CNN), leveraging hyper-convolution and capsule layers to capture complex spatial hierarchies.

B. Paper Organization

Section I introduces cancer with a related discussion, Section II about a Literature review on skin cancer, various machine approaches with classification techniques, and performance metrics. Section III discusses the methods of the proposed APSIO classification algorithm for skin disease identification. Section IV presents a comparison analysis of the proposed HCI-CNN algorithm, and a discussion of metrics calculation with output is provided. In Section V, the study's conclusion and submissions of skin cancer classification processes are presented.

II. Literature Review

A computerized approach to skin disease classification using Long Short-Term Memory (LSTM) and Mobile Net V2, based on deep learning. The Grey-Level Co-occurrence Matrix (GLCM) utilizes the recurrent pattern of the localized intensity factor. The color and strength of a pixel are determined by the GLCM's spatial distribution based on the distribution of intensity levels. The ReLu6 module [6] is used in the output of the third layer.

A secondary deep learning network is used in conjunction with an experimental multimodal smartphone imaging technique that produces RGB and fluorescence images. The fluorescence-aided amplification network (FAA-Net) is used to identify skin conditions. FAA-Net [7] was revised with an attention mechanism module to detect skin disease locations autonomously and mark potential disease regions.

The use of human skin as a basis for these models enables self-learning algorithms to operate effectively. ANNs are neurons (nodes) connected [8] at various levels, such as brain cells in biology. In a network of neurons, data is stored, processed, and output. The CNN approach requires extensive recurrent training, and an ample image database had to be used to mitigate the risk of over-fitting.

The FAA-Net is now equipped with an attention module that automatically detects skin disease sites and marks potential disease regions. According to experimental results [9], the average accuracy and area under the curve of our produced model for detecting skin diseases were 8.61% and 9.83%, respectively.

The methods used high-resolution dermoscopic images to identify skin conditions, including psoriasis, dermatitis, and melanoma. The growing availability of large annotated image datasets has accelerated the development of this classification. Edge detection and segmentation techniques are frequently used to extract Regions of Interest (ROIs) [10], such as lesions or impacted regions. With an accuracy of 91.2%, the K-Nearest Neighbor classification algorithm outperforms the SVM classification method.

The modified single DCNN model method [11] employed Modified R, Augment, MWNL, and CLS to achieve classification accuracy on certain dermoscopic image datasets that was at least as good as, or superior to, that of many ensemble methods. For optimal performance, a Fully Fused Network (FFN) is composed of an Improved Single Block (ISB) and an Improved Fusion Block (IFB) [12].

An attention-mixing decoder and multi-axis encoder were utilized in an attention-based, encoder-decoder architecture to segment the skin layers accurately. The simulation successfully maintained both global and local features using a transformer-based encoder block. These features were then sent to the decoder block via an attention-based controlled skip link. By employing vision transformer structures [13], the multi-axis encoder enables the encoding of feature representations at various scales. The self-attention mechanism of transformers enables medical image segmentation to achieve remarkably high accuracies while accommodating dependencies over extended periods.

Skin images saved in a data format on the blockchain are used to categorize skin conditions. Here, segmentation is performed using Deep Joint Segmentation, which has been modified by the introduction of the Kumar-HasseBrooks distance [14] and Transit Circle Inspired Optimization-LENet, achieving an accuracy of 0.92 and a True Positive Rate of 0.93.

A DL architecture, described as Swin Transformer, was created for image categorization. This network's input is divided into non-overlapping windows using a hierarchical method. Fine-grained spatial characteristics are essential for precise classification. The final output probabilities [15] for each class were generated by processing the concatenated features through a fully connected top layer. The focused loss of the predicted class probabilities relative to the target class is maximized to optimize the network parameters.

Pre-processing injury segmentation and classification are crucial steps in the proposed classification approach. After image pre-processing, skin lesion segmentation was accomplished using improved U-Net segmentation [16], which achieved this enhancement by proposing a hybrid optimization approach. The spatial interdependence between image areas is achieved without the need for substantial pre-processing or the use of constants, utilising features and leveraging the self-attention mechanism of transformer models. A thorough analysis of many Deep Learning models [17] using reference datasets for skin imaging for different skin lesions. The model was trained when the number of training images and large datasets increased, and it was created by combining smaller datasets, achieving a test accuracy of 86.37%.

A deep learning-based model for skin cancer detection was developed using a transfer learning approach [18], effectively distinguishing between benign and malignant stages. For classification of skin diseases, an ensemble of enhanced convolutional neural networks (CNNs) was employed in conjunction with a test-time augmentation strategy known as frequently spaced shifting [19]. The CNN model was evaluated using 960 images from the ISIC 2018 Skin Lesion Classification Challenge test set, which included 360 benign and 300 malignant images [20]. The complete dataset comprised 3,533

lesion scans, nearly balanced with 1,760 benign and 1,773 malignant samples. To capture multi-scale features, the Inception architecture was utilized, leveraging multiple convolutional kernels with diverse receptive fields to extract features at different spatial resolutions.

A clinical decision support model [21] for skin disease detection and classification using a hybrid deep learning approach and enhanced segmentation capabilities. The tests related to data dimensionality were handled using Multi-Strategy Seeking optimization (MSSO), which optimizes feature selection by determining the essential characteristics of hand and High-dimensional data using the Multi-Strategy Seeker Optimization (MSSO) approach.

A complex neural network model [22] can automatically identify and differentiate between several types of skin lesions using dermoscopic images. Deep learning, particularly CNN, which learns hierarchical representations directly from raw image data, enables accurate feature extraction. This approach reduces the need for human feature engineering while increasing diagnostic accuracy. The algorithm is trained on large annotated datasets to classify lesions as benign or malignant, and then further categorize them into specific cancer subtypes.

An algorithm based on dermoscopic images with channel-specific, channel-shared, and depth-related variables. The Transformer baseline model [23], the traditional CNN model, and two datasets were evaluated against a dataset of Minnesota dermoscopic images, and the average accuracy of 70.23%. Training and validation loss, training and validation accuracy, as well as confusion matrices for each of the six networks that used transfer learning, were compared [24]. The objective was to expand the filter bank dimension before adding it to match the input depth.

EfficientNetB0 [25] through transfer learning to enhance melanoma detection. Their approach yielded high diagnostic accuracy while maintaining computational efficiency, making it suitable for deployment in mobile health systems. However, the study focused solely on melanoma, limiting its applicability in multi-class skin disease classification. Introduced a hybrid ensemble model combining DenseNet and MobileNet [26]. Their deep learning ensemble improved classification robustness and generalization across different cancer types, although the increased model complexity resulted in higher training overhead.

A fine-tuned DenseNet-121 model to classify skin lesions with improved feature reuse and gradient flow, achieving reliable results for binary classification tasks [27]. Ensemble learning by integrating multiple CNN architectures [28], which significantly boosted sensitivity and specificity. The effectiveness of traditional machine learning classifiers in detecting skin cancer using handcrafted features [29]. Their comparative study involving classifiers such as SVM, RF, KNN, and Naïve Bayes concluded that the Random Forest model offered superior accuracy. Though their work highlights the value of ML in dermatological diagnostics, it also emphasizes the limitations of manual feature engineering, pointing to deep learning as a promising direction for future research.

The application of transfer learning using deep CNN architectures, including VGG16, ResNet50, and DenseNet201, for classifying skin cancer lesions [30]. Utilizing the ISIC dataset and augmentation techniques, they achieved high classification accuracy, particularly with ResNet50. Their findings underscore the efficacy of deep learning models for dermatological diagnostics and highlight transfer learning as a robust strategy for medical image analysis with limited labeled data.

A lightweight CNN model tailored for cloud-based and mobile applications in skin cancer diagnosis [31]. Using the ISIC dataset, the model achieved competitive accuracy while maintaining low computational demands, enabling real-time analysis in remote or resource-limited settings. Their approach presents a viable solution for scaling dermatological services via telemedicine. The model effectively distinguished between seven different lesion types and achieved over 89% accuracy [32]. Their work underscores the strength of CNNs in handling complex dermatological image classification tasks beyond binary diagnosis, although class imbalance remains a challenge.

A MobileNet-based lightweight deep learning model [33] for seven-way skin lesion classification using the HAM10000 dataset. The system supports real-time, on-device predictions, demonstrating strong potential for deployment in tele-dermatology and low-resource environments.

The HAM10000 dataset, train a model for classifying skin cancer, training and validation losses, training and validation accuracies, and confusion matrices of every one of the six transfer learning networks carried out with the matching complexity of the inputs by augmenting the dimension of the filter before adding.

A. *Problems Identified*

Despite significant advancements in approaches for automating the detection of skin diseases using machine learning and deep learning methodologies, existing approaches tend not to optimize for classification accuracy and computational efficiency in real-time applications. Additionally, most existing research does not incorporate feature selection, segmentation, and classification. In this review, various types of skin cancer datasets and different performance analysis outputs are discussed. However, some limitations of this survey were identified from the review analysis in previous research work. Table I, literature survey discusses the gaps and reviews deep learning and machine learning algorithms for identifying skin diseases.

B. *Research Contribution*

- Development of an AI-powered skin disease detection framework that integrates preprocessing, clustering, segmentation, feature selection, and classification tailored for diverse skin tones and dermatological conditions.

TABLE I. PROBLEM DESCRIPTION OF SKIN DISEASES IDENTIFICATION

Ref	Algorithm Used	Output	Dataset	Gaps
[25]	Rectified Adam (RAdam)	F1 Score 88 % Recall 88 % Precision 89 %	HAM10000 dataset	Negatively impacted by overfitting in small or unbalanced classes.
[26]	CNN	accuracy 93.75%	ISIC dataset	Demand fine-tuning of hyperparameters and substantial computational resources.
[27]	DENSENET-121	accuracy 87%	HAM10000 dataset	Low data or poor image quality can cause performance to deteriorate.
[28]	CNN	accuracy 92.16%	HAM10000 dataset	Limited generalization across lesion types without data augmentation
[29]	Particle Swarm Optimization (PSO)	accuracy 86.9%	Kaggle dataset	Performance and convergence rate are strongly influenced by initial parameters.
[30]	Transfer Learning (ResNet50, InceptionV3, DenseNet201)	Accuracy >90%,	ISIC Dataset	Does not include segmentation; performance depends on pre-trained model and dataset quality
[31]	Custom lightweight CNN	Accuracy >87%	ISIC Dataset	Limited feature extraction compared to deeper models; no segmentation included
[32]	Custom Deep CNN	Accuracy >89%	HAM10000	Lacks integration with segmentation tools
[33]	MobileNet (lightweight CNN)	Accuracy >85%	HAM10000	May underperform on rare or ambiguous lesions; real-time use tested only in prototype

- A new AI-driven methodology for skin disease diagnosis using APSIO feature selection combined with a hybrid YOLO and HCI-CNN model.
- Application of APSIO feature selection, which effectively reduces computational complexity and false positives, ensuring optimal feature relevance and improving diagnostic accuracy.
- Robust segmentation approach for extracting geometric and physical attributes of skin lesions, facilitating precise evaluation of lesion boundaries and types of damage.
- Enhanced image preprocessing pipeline designed to improve clarity and contrast for a range of skin tones, contributing to fairness and inclusivity in dermatological AI applications.
- Potential for integration into real-time medical diagnostic tools, providing support for healthcare professionals in clinical environments, leading to faster diagnosis and improved patient outcomes.

This proposed work focused on a hybrid intelligent architecture that includes APSIO feature optimization and an ensemble prediction model using deep learning models, allowing for better diagnostic accuracy while being applicable in real time.

III. PROPOSED METHODOLOGY

A skin disease classification structure based on HCI-CNN to maximize classification performance and improve feature selection. Pre-processing enhances the quality of images and highlights significant patterns; the skin images extracted are pre-processed through a Gaussian wavelet transform, efficiently enhancing discriminative patterns and enhancing the quality of follow-up analysis. Segmentation technique with Weighted Strategy (SFWS) segments specific skin layers and regions of interest in classification. APSIO Feature selection adaptively controls evaluation parameters during training, allowing real-time adaptation and offline optimization. This process selects the most informative and relevant features for effective classification. High-level discriminative patterns are initially derived from medical skin images using HCI-CNN with YOLO classifying features and are tested through layers to classify into several diseases, Melanoma, Basal Cell Carcinoma (BCC), Actinic keratosis, Melanocytic nevi, Benign keratosis, Vascular lesions, and Dermatofibroma. If no dermatological abnormalities are detected in the collected clinical skin image, the system will classify it as normal skin. Fig. 1 shows a block diagram of the proposed method; a complete description of each block is mentioned below.

A. Gaussian Wavelet Spectral Filter (GWSF) Preprocessing

GWSF Filter, image pre-processing process calculates the weights of the Gaussian smoothing, the weights of the wavelet transform, and the scalar values to enhance the features of skin images or avoid noise effectively, and not let the edge information be analyzed over during the process. Small image noise from a whole image and keep large structures in that image, untouched process validates large image structures that are preserved by discarding a small image with multi-resolution must be performed.

$$h(m,n) = \frac{1}{2\pi\,\sigma^2}\, e^{-(m^3+n^2)\,/\,2\,\sigma^2} \quad (1)$$

Eq. (1), σ characterizes the distribution's standard deviation, and the distribution's mean is taken to be 0.

$$H\,(U,V) \;\approx\; e^{-2\,\pi^2\,\sigma^2\,(u^2+v^2\,)} \quad \text{for } |U|,|v| < \frac{1}{2} (2)$$

Eq. (2), $H\,(U,V)$ Impulse response and occurrence reaction both gradually decrease, and the Gaussian filter stands out for not leaking noise or distorting.

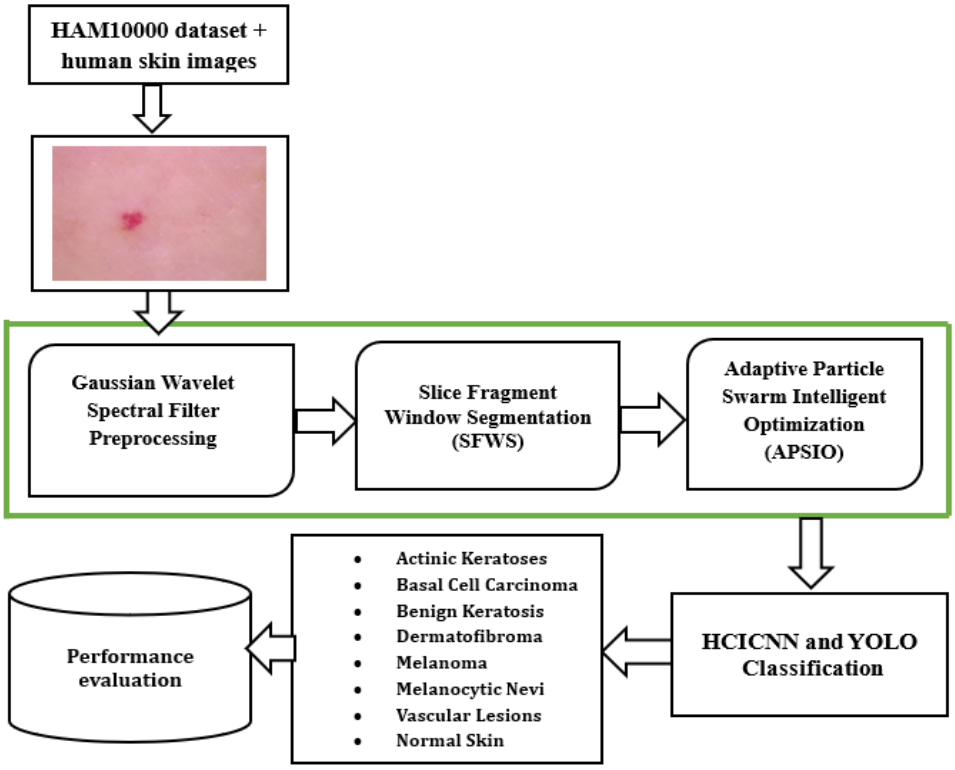

Fig. 1. Overall proposed diagram.

$$I = \int_{-\infty}^{\infty} \exp(-x^2)\, dx = \sqrt{\pi} \qquad (3)$$

Eq. (3), when changing I represents negative to positive values, dx describes the complex error of the possible values in any given space in probabilistic terms.

$$hxy = fxy \odot wxy \qquad (4)$$

Eq. (4) wavelet domain GWSF filtering improves complex structures as dark skin surface, texture patterns, border anomalies, and inhibits already spent data. Combining the two steps results in a preprocessed image, retains diagnostically relevant structures with improved contrast and less noise. It is also especially useful for analyzing affected skin areas, which improves the signal-to-noise ratio and feature stability across samples, leading to improved overview and classification performance in skin analysis. Fig. 2 shows the input skin cancer images and the GWSF filtering images output.

B. Slice Fragment Window Segmentation (SFWS)

SFWS is a progressive technique considered to improve the segmentation area of skin disease areas in medical images, particularly skin dataset images. The algorithm works by separating. The input image into reduced manageable fragments or "slices" using a sliding window method. Each window captures localized image data, preserving the spatial context and fine-grained texture differences of skin cancer. The cluster area is separated by specific regions, inner and outer border detection, particularly in cases of irregularly shaped or low-contrast skin affected. By leveraging contextual signals and SFWS can efficiently differentiate between normally affected skin and diseased regions, even in complex background conditions.

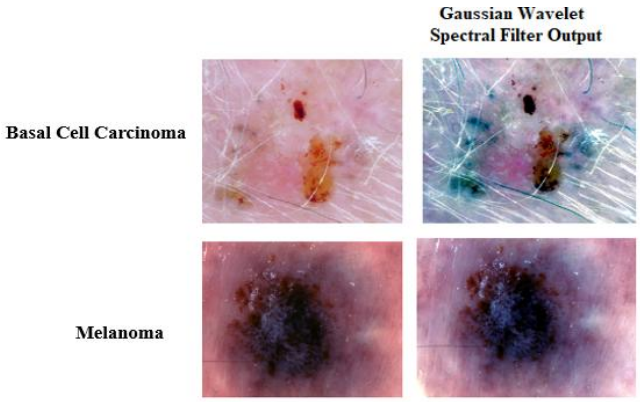

Fig. 2. GWSF preprocessing output.

$$S = S_{cls} + S_{box} + S_{max} \qquad (5)$$

In Eq. (5) S_{cls} specifies the skin affected area, and k_{box} indicates the outer region of the affected skin.

$$Scs\ (q, v) = -\log e\, V \qquad (6)$$

In Eq. (6), V specifies the object class q = $(q_o\ , \ldots\ldots\ldots . q_k)$ using a logical function.

$$I\ (x) = \arg\max\ (A(x), B\ (x)) \qquad (7)$$

In Eq. (7), segmentations of all the skin layers are multipart to reproduce the whole segmented image.

$$a\ (x, y) = \frac{1}{th} * \sum_{s=-a}^{a} \sum_{t=-b}^{b} f(x + o\ , y + i) * f(x + o\ , y + i) \qquad (8)$$

In Eq. (8), o and i represent the dimensions of the over skin pixel.

$$l\,(E_k) = \sum_{k=0}^{n-1} p\,(r_k) \tag{9}$$

Eq. (9) is adjusted to the adjoining rate after being augmented by L1 indirection to control the pixel's value.

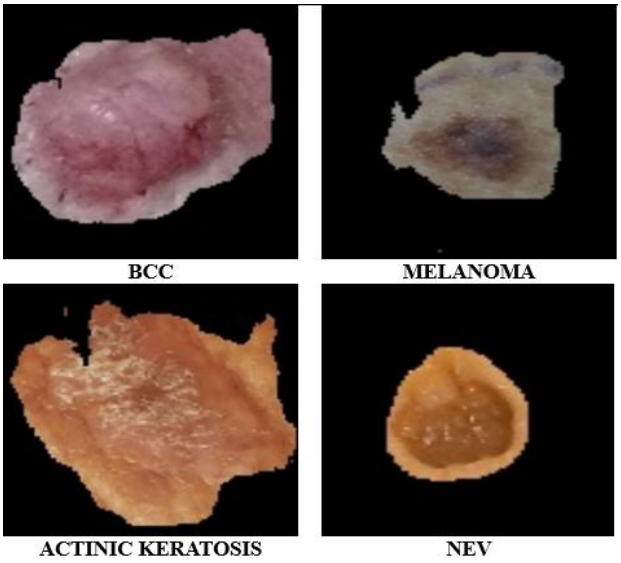

Fig. 3. SFWS segmentation output.

Fig. 3 shows the overlapping objects and variations caused by the segmentation approach as common pixel, weighted average, or confidence-based overlap segment selection. This technique is specifically valuable in processing images of high size and resolution without the need to downscale, typically resulting in information loss. Its networked context also makes it suitable for deep learning models, contributes towards more correct and stable subdivision, supporting dermatologists in early and accurate detection of skin diseases.

C. Adaptive Particle Swarm Intelligent Optimization (APSIO) Feature Selection

APSIO is a feature selection procedure that aims to select the most relevant features from a dataset for use in structure and training. The APSIO calculates the potential of each feature and assigns a fixed binary or continuous vector to each subset, adjusting its position based on the pixel of each skin layer. The adaptive approach dynamically changes the acceleration coefficients, inertia, and weight based on the current performance, range, and iteration progress of the swarm. The dataset is split into an 80:20 ratio, with 20% kept back for testing, and the remaining 80% used for training. Fig. 4 shows the working flow. APSIO takes input data features such as numerical or categorical parameters of the dataset, which are first preprocessed and normalized. Feature range is done by an adaptive mechanism that assesses each feature's relevance as per fitness scores obtained from a predefined objective function. Every particle in the swarm is a candidate solution, a set of features with position and velocity being updated step by step. The algorithm estimates the fitness of every particle by measuring model performance (e.g., classification accuracy or error rate) based on the chosen features.

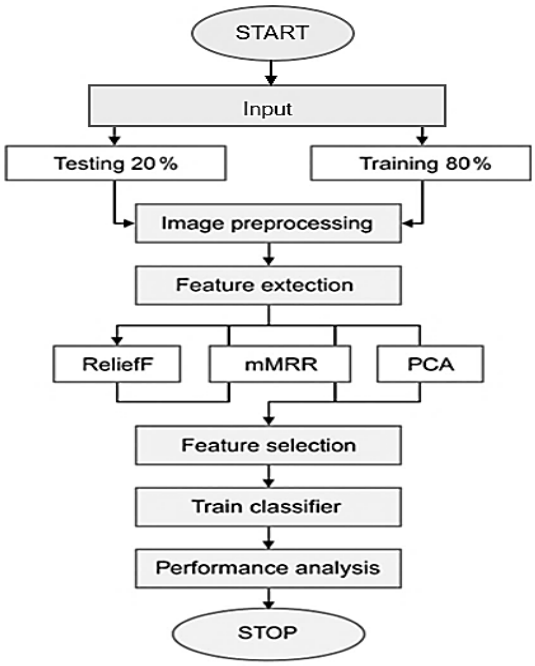

Fig. 4. Flow chart of APSIO feature selection.

Adaptive methods update particle behavior according to convergence trends dynamically, optimizing an exploration and exploitation balance. The result is the optimal subset of features that maximizes the objective function, enhancing the performance, and minimizing dimensionality.

D. APSIO Algorithm

1) Adaptive inertia weight in particle velocity update

$$v_i^{(t+1)} = w^{(t)}.v_i^{(t)} + C_1.r1.\left(p_i^{best} - x_i^{(t)}\right) + c2.r2.\left(g^{best} - x_i^{(t)}\right) \tag{10}$$

In Eq. (10), $v_i^{(t)}$ rate of unit i at iteration, $w^{(t)}$ adaptive inertia weight (variations per iteration) for calculating the features.

2) Position particle update

$$x_i^{(t+1)} = x_i^{(t)} + V_i^{(t+1)} \tag{11}$$

In Eq. (11), $(t+1)$that creates a binary representation (0 or 1) from a constant search space, where procedures may examine various feature combinations.

3) Determine each element's fitness using a few chosen structures

$$S\left(V_i^{(t)}\right) = \frac{1}{1+e^{-v_i^{(t)}}} \tag{12}$$

In Eq. (12), A Binary Transfer Function (BTF) $S\left(V_i^{(t)}\right)$, a mapping used in the selection of features which ends up in a binary representation (0 or 1) for each feature, signifying its inclusion or exclusion in the chosen subset, from a continuous search space where procedures may examine various feature configurations.

4) Function of binary transfer (for feature selection)

$$x_i^{(t+1)} = \begin{cases} 1 & if\ r < S\,V_i^{(t)} \\ 0 & otherwise \end{cases} \quad (13)$$

In Eq. (13), feature subset valuation of a fitness function is a numerical appearance, which calculates how well a detailed feature subset is suitable for classification. At different selecting features, a collective skin structure image that shows the continuing link is created by reflecting of essential perceptual uniform areas.

5) Optimization and backpropagation: Every few iterations, backpropagation can be used to optimize selective parameters.

$$x_i = x_i - \eta \nabla_x L(x_i) \quad (14)$$

In Eq. (14), η denotes the learning rate, and $\nabla_x L$ represents the gradient of the loss function with respect to the weights and biases denoted by x_i.

6) Output: An optimized binary vector $x_i \in \{0,1\}^n$ for each particle, representing the selected feature subset.

E. Hyper-Convoluted Intra-Capsuled Neural Network (HCI-CNN) and YOLO Algorithm

The HCI-CNN structure utilizes hyper-convolutional layers to identify complex spatial pixels and employs capsule-based learning to preserve the pose and structural relationships between different layers of skin. In the initial stage, a convolutional layer with 32 filters of 3×3 and ReLU activation is utilized to extract low-level visual features. To ensure efficient and stable training, an exponential moving average with a momentum of 0.99 is implemented, along with an adaptive learning rate of 0.001.

Fig. 5 shows the detailed architecture of the proposed hybrid classification model in skin disease detection.

The HCI-CNN and YOLO algorithms operate in a hybrid manner by integrating deep feature extraction and real-time object detection. HCI-CNN accepts preprocessed dermoscopic images and clinical images as input and uses hyper-convoluted layers to extract detailed texture, color, and structural features, which are encoded through intra-capsuled routing mechanisms for high-level representation. Such encoded features are used for the classification of skin lesions with high accuracy.

At the same time, the YOLO algorithm classifies the same images to identify and locate infected skin areas by segmenting them into a grid and predicting bounding boxes and confidence estimates. The hybrid system leverages HCI-CNN's classification power and YOLO's spatial localization feature. The combined technique improves both diagnostic accuracy and detection efficiency in medical imaging tasks. The Hybrid HCI-CNN and YOLO classification technique aims to enhance the accuracy of skin disease classification using medical images.

Fig. 6 shows an intra-capsuled architecture, which continues layers and orientation information through dynamic routing units, enabling the model to maintain spatial relationships among structures. As an outcome of HCI-CNN surpasses conventional CNNs by achieving greater generalizability, coupled with improved handling of intricate skin disease contours in diagnostic contexts.

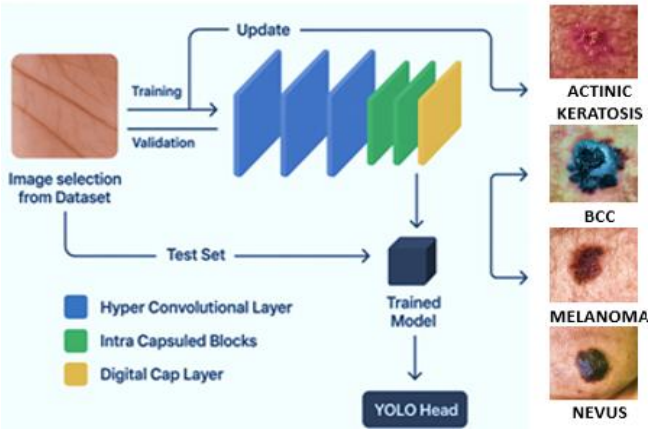

Fig. 5. Hybrid architecture diagram of HCI-CNN and YOLO algorithms.

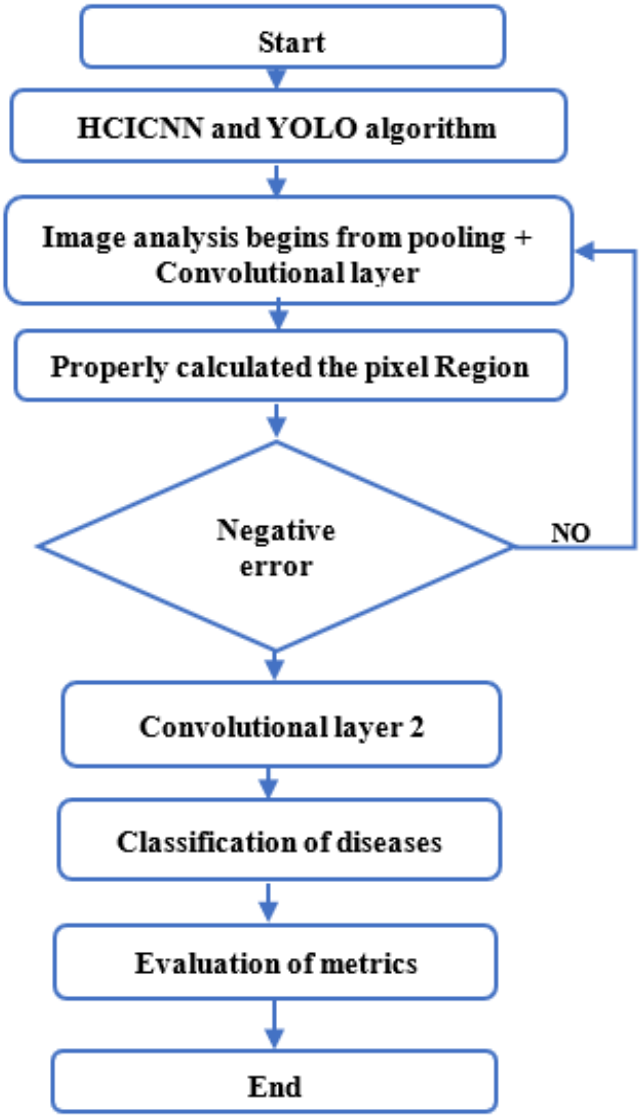

Fig. 6. Flow chart of feature classification.

F. Hybrid HCI-CNN and YOLO Algorithm

1) Convolution hyper layer

$$Y = \sum_{i=1}^{C_{in}} k_i\,(x) * x_i \tag{15}$$

In Eq. (15), x is an input mapping channel, $k_i\,(x)$ is dynamically evaluated for pixel classification.

$$d_e\,(x,y) = \sqrt{\sum_{n-1}^{n}(x_i - y_i)^2} \tag{16}$$

In Eq. (16), distance n is probably the most frequently used distance of difference across feature vectors. Here n represents the number of characteristics.

$$d_e\,(x,y) = \sum_{i=1}^{n} |\, a_{i-}\, b_i\,| \tag{17}$$

In Eq. (17), (a,b) constant may be used to quantify the separability of classes and to determine closely two samples (x,y), under the different skin classes are related.

$$e\,[\,X\,,Y\,] = \frac{1}{N}\sum_i X_i - Y_i \tag{18}$$

In Eq. (18), hyper-convolutional layers $X_i - Y_i$ are evaluated using multi-scale receptive field processing to capture both fine-grained texture and contextual information, enabling the differentiation of visually confusable skin cancer types.

Apply the YOLO Classification algorithm to predict object boundaries and class labels

In Eq. (19), each pixel within the region is characterized based on the amount of associated data.

$$X_O = X_1 + X_2 + X_3 \tag{19}$$

2) Capsule intra transformation

- Approach Routing ($U_{i,j}\,, r,\ l$), All capsules I and J in layer l and (l + 1), respectively.
- for r iterations, do
- for all capsule i in layer l: $C_i = softmax\,(b_i)$
- for all capsule j in layer (l + 1): $S_j = \sum_{i=1}^{N} C_{i,j}\,, U_{i,j}$
- for all capsule j in layer (l + 1): $V_j = Squash\ S_{i,j}$

3) Routing between capsules in a dynamic manner: In Eq. (20), a squash function is applied to normalize the output vectors of capsules.

$$V_j = Squash\,(\sum_i cij\ u\ j|\ i) \tag{20}$$

4) Output: The vector magnitude is maintained between 0 and 1 by using the nonlinear squashing function, evaluated in Eq. (21)

$$P\,(y = k\,|\,x\,) = |V_k| \tag{21}$$

IV. Results and Discussion

Skin disease identification is the basis for the experiment calculation, and the system uses a specific dataset from which performance analysis is assessed. The specific test data with predictive values is properly evaluated for feature selection, identification of specific skin conditions, and comparison with previous studies. The APSIO feature selection and HCI-CNN classification are evaluated in this result and discussion.

A. Skin Diseases Dataset Description

The proposed method uses a dataset of high-resolution clinical skin images using the recommended medical application, 10015 images representing seven different classes includes Melanocytic Nevi (6705), Melanoma (1113), Benign Keratosis (1099), Basal Cell Carcinoma (514), Actinic Keratosis (327), Vascular Lesions (142), Dermatofibroma (115) from the HAM10000 dataset and it can be gain from https://www.kaggle.com/ and 1200 clinical images which is collected from individuals. Each image is associated with specific attributes. The dataset is divided into seven categories of dermoscopic images. The images are split into a training set (80%) and a testing set (20%).

B. Feature Selection Calculation

Three feature selection methods are compared in Table II based on feature dimensionality, computational time, and accuracy. When compared based on skin image features, the proposed APSIO method demonstrated superior performance, achieving higher accuracy than other methods across different data volumes. These results demonstrate that APSIO is a highly effective optimization-based feature selection technique, achieving higher accuracy with significantly fewer features and making it well-suited for efficient and accurate skin image classification tasks.

TABLE I COMPARATIVE ANALYSIS OF SKIN FEATURE SELECTION METHODS

Feature Selection	Computational Time (s)	Feature Dimensionality	Accuracy
Histogram of Oriented Gradients (HOG)	1.8	High (~3780 features/image)	92.4
Gray Level Co-occurrence Matrix (GLCM)	1.2	Medium (~20–40 features)	94.3
Adaptive Particle Swarm Intelligent Optimization (APSIO)	2.4	Low (~10–15 optimized features)	95.3

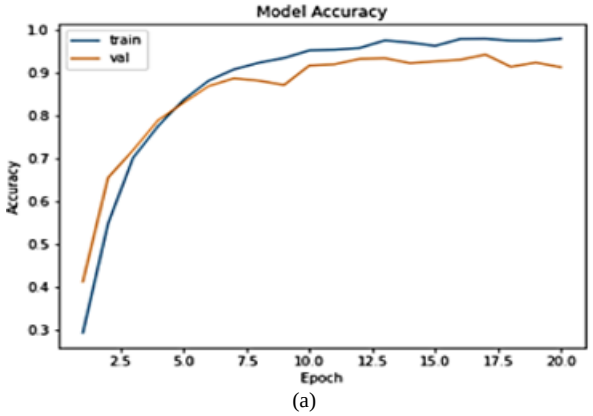

(a)

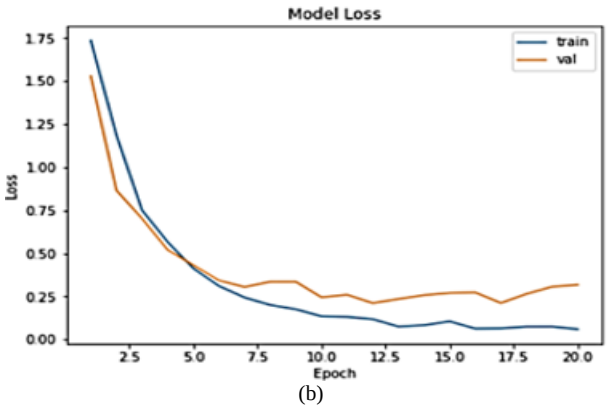

Fig. 7. Training and testing accuracy and loss.

Fig. 7 shows the accuracy of the typical and the loss of the APSIO approach generated from segmented images. The highest value of loss is 1.75, and the value decreases, as indicated by (a), as epochs increase, as indicated by (b). The output of the Dense model performs best on the testing set using segmented images.

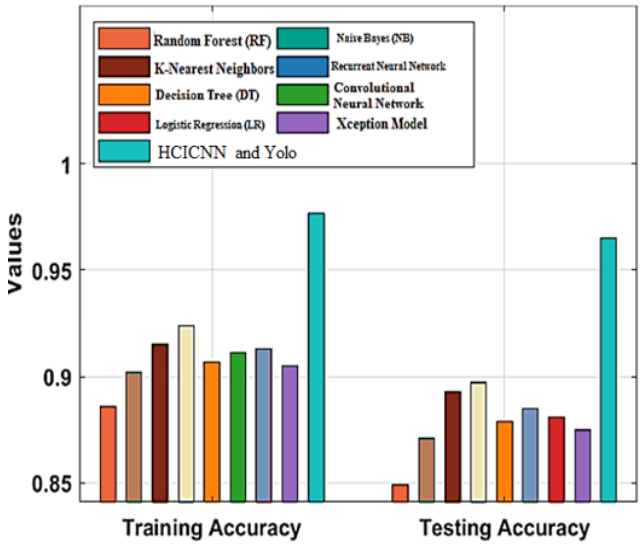

Fig. 8. Training and testing accuracy of hybrid HCI-CNN and YOLO.

Fig. 8 evaluates and compares the performance of different deep learning and machine learning models for classification problems. In terms of generalization, the Hybrid HCI-CNN and YOLO models achieve higher accuracy than the previous classification methods.

C. Experimental Evaluation

The Error-Level Analysis (ELA) in Fig. 9 evaluates the error rates of different classification outputs. The HCI-CNN had a reduced error rate of 5.5%, which was significantly lower than GoogLe-Net 14.3%, ResNet 13.2%, and Mobile Net 8.4% and demonstrates the superior performance of HCI-CNN compared to other models.

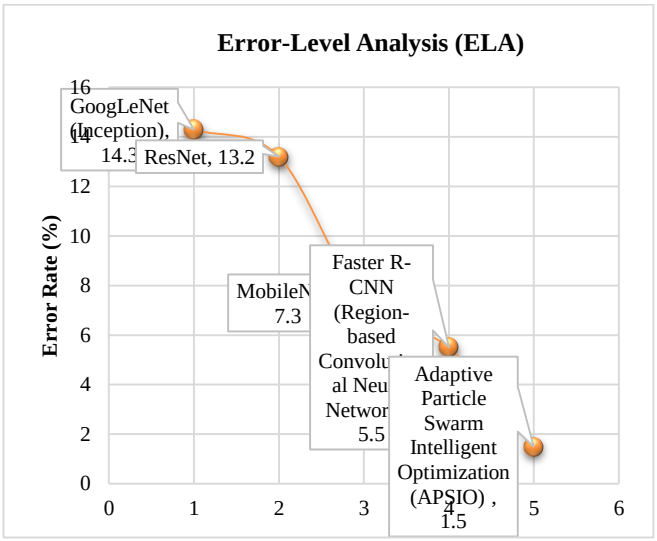

Fig. 9. Error rate analysis.

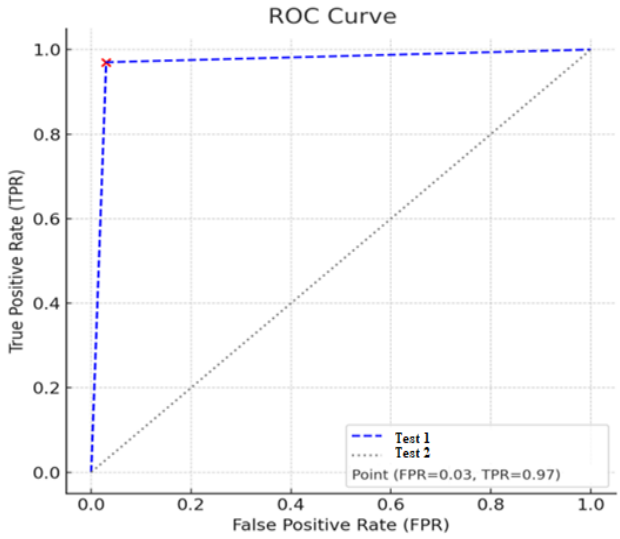

Fig. 10. HCI-CNN classification ROC curve.

Fig. 10 shows the HCI-CNN classification error analysis based on the test data, indicating a True Positive Rate (TPR) of 0.97 and a False Positive Rate (FPR) of 0.03.

D. Comparison Evaluation

Fig. 11 validates that the proposed hybrid approach, HCI-CNN combined with YOLO, reaches a maximum accuracy of 97%, which is significantly better than the previous ResNet50 and K-nearest neighbour, which show accuracies of 94 %, ResNet101V2 accuracy of 86 %.

Fig. 12 shows that the HCI-CNN and YOLO hybrid model significantly improves recall, achieving 96.55% compared to existing methods. Random Forest and SVM achieved recall values of approximately 82.5% and 88.3%, respectively, whereas ResNet achieved 89.3% and Extreme Gradient Boosting achieved 92.5%.

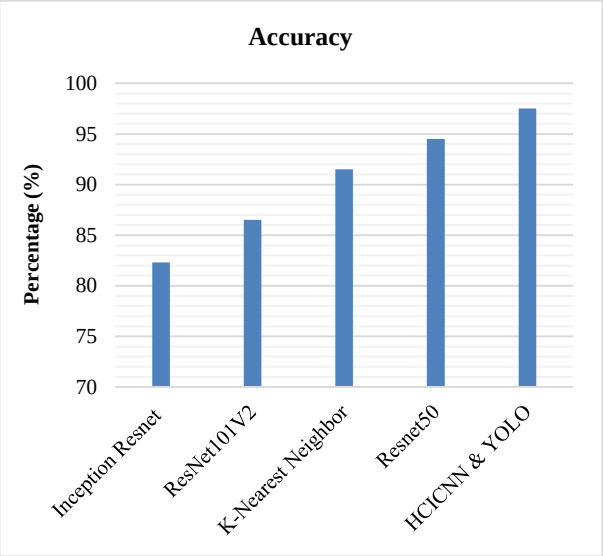

Fig. 11. Proposed classification accuracy analysis.

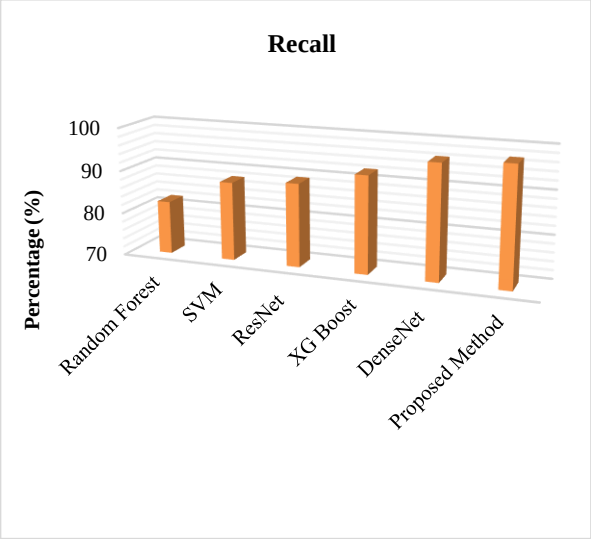

Fig. 12. Proposed recall analysis.

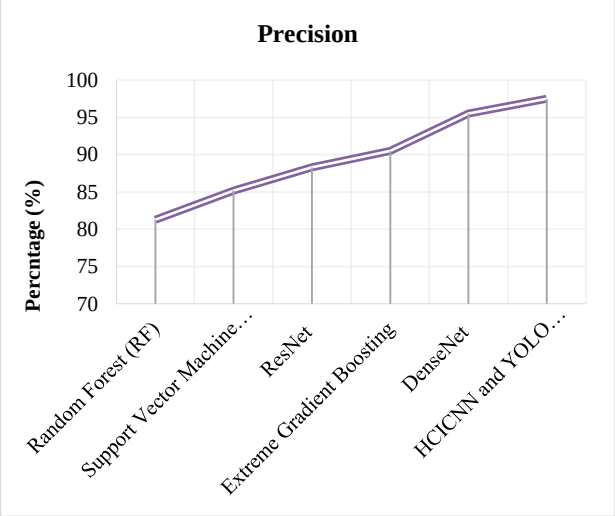

Fig. 13. Proposed precision analysis.

Fig. 13 shows that the proposed HCI-CNN and YOLO method achieves a precision of 96.52%, outperforming other existing methods such as Random Forest (81.3%), SVM (85.2%), ResNet (88.4%), and Dense Net (95.6%).

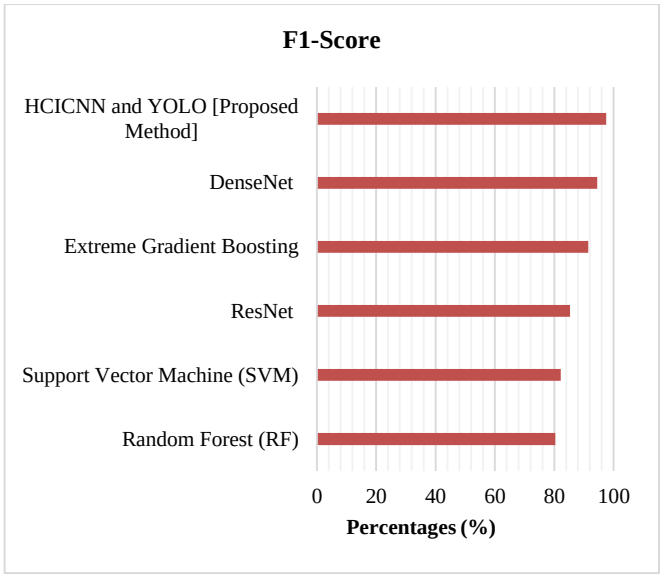

Fig. 14. Proposed F1-score analysis.

Fig. 14 shows a comparison graph of F1-Scores for various machine learning models, including Random Forest and SVM, which demonstrate an average performance of 83%. However, deep learning models such as deep residual networks and eXtreme Gradient Boosting are also compared. The proposed HCI-CNN and YOLO methods are also compared, with the highest F1 score of 96.93% achieved by HCI-CNN, demonstrating its superior performance.

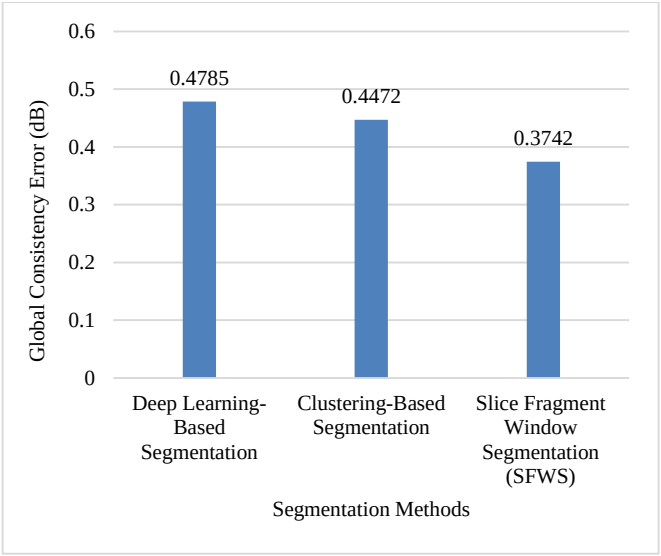

Fig. 15. Proposed segmentation analysis.

Fig. 15 shows the segmentation evaluation of Global Consistency Error (dB) across the three segmentation methods: Slice Fragment Window Segmentation (SFWS), Deep Learning-Based Segmentation, and Clustering-Based Segmentation. The proposed SFWS has the lowest error at

0.3742 dB, demonstrating the highest reliability. In contrast, the Deep Learning-Based Segmentation has an error of 0.4785 dB, followed by the Clustering-Based Segmentation with an error of 0.4472 dB.

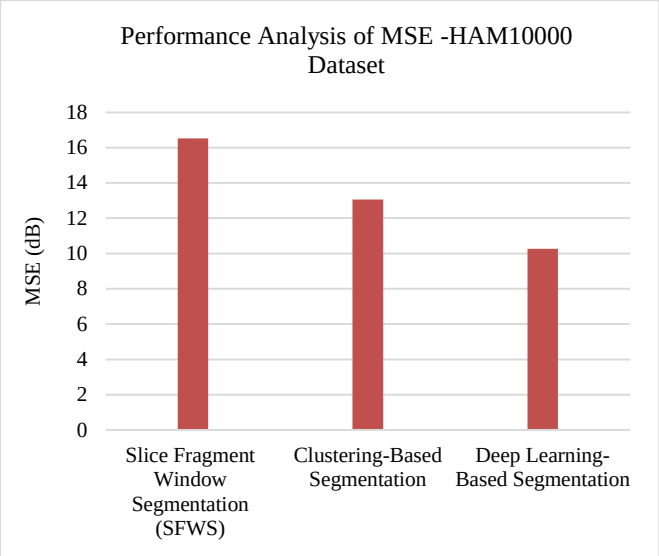

Fig. 16. MSE segmentation comparison analysis.

In Fig. 16 MSE (Mean Square Error) for skin image segmentation with the existing approach is evaluated through the proposed SFWS method as an improved segmentation analysis.

Fig. 17 illustrates the analysis results of the collected clinical skin images. When no dermatological abnormalities are detected in the collected clinical skin image, the system classifies it as normal skin; otherwise, it is classified as a disordered image. Among the 1,200 clinical skin images evaluated, 1,194 were detected as normal, and the remaining 6 were identified as containing dermatological disorders.

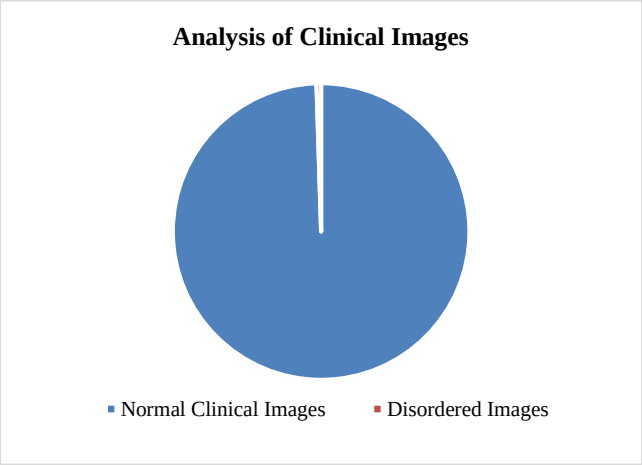

Fig. 17. Assessment of acquired dermatological images.

Table III presents a comparative analysis based on four different parameters, using data from cited references that support the comparison technique.

TABLE II COMPARISON OF EXISTING SKIN CANCER IDENTIFICATION METHODS

References	Accuracy (%)	Precision (%)	Recall (%)	F1-Score (%)
Ashtagi et al. [25]	91.50	91.00	90.00	90.50
Imam et al. [26]	93.75	93.75	92.50	93.00
Bello et al. [27]	87.00	87.00	86.00	86.50
Khan et al. [28]	92.16	92.16	91.50	91.80
Natha et al. [29]	86.90	86.90	85.50	86.00
Jain et al. [30]	90.00	90.00	90.00	90.00
Huang et al. [31]	87.00	87.00	86.00	86.00
Chaturvedi et al. [32]	89.00	89.00	88.00	88.00
Gupta et al. [33]	85.00	85.00	84.00	84.00
Proposed Model	**97**	**96.52**	**96.55**	**96.93**

E. Discussion

Specific AI technologies have a significant impact on reliability and diagnostic classification results for classifying skin disease. In this research work, HCI-CNN and YOLO are applied for classification, while APSIO is employed for feature selection. The combination of these procedures addresses critical tests such as high-dimensional data, feature idleness, and demand for amplified classification accuracy. The mechanism of APSIO dynamically adjusts the limits of the convergence rate. The most discriminative features are selected from dermoscopic images owing to this adaptive mechanism, which decreases computational difficulty without compromising diagnostic accuracy. Deep and wide convolutional layers with multiple levels of abstraction constitute the HCI-CNN architecture, which is effective in capturing.

V. CONCLUSION

The proposed AI-powered skin disease detection method utilizes advanced image processing techniques, including preprocessing, clustering, and classification. Through the preprocessing filter, the image improves in clarity for different skin colors. In segmentation, factors are divided to evaluate geometric and physical damage. In APSIO feature selection, related features are selected. Furthermore, a hybrid approach integrating HCI-CNN and YOLO is employed for effective classification. This approach demonstrates high accuracy in the detection and classification of seven different types of skin disorders. The selective features remove false positives and computational burden, with the added potential for real-time medical applications. In this study, both real-world clinical images from individuals and curated images from established datasets were analyzed to evaluate the system's performance comprehensively. The output performance analysis, with an Accuracy of 97%, a precision of 96.52%, a recall of 96.55%, and an F1-score of 96.93%, will enhance performance and improve classification for applications in healthcare facilities, ultimately leading to improved treatment outcomes for patients with skin diseases.

In the future, the rising plurality and complexity of skin diseases require new modalities with newly available technologies, such as AI and the IoT, to better align and sustain

the management (exposure reduction) of skin diseases. IoT-based wearables equipped with high-fidelity imaging sensors and biosensors can continuously monitor skin surface indicators, temperature, and moisture, as well as the evolution of skin lesions, enabling direct and real-time examination of skin health by identifying the reliable amount of surface data on a person. Combining this data with an AI analytical model, which leverages streaming and real-time data, enables humane dimension management (e.g., tracking behaviors, detecting anomalies, and risk stratification) while learning and evolving. Future directions for connected wearables in regulating dermatological diseases can be supported by hybrid frameworks of learning, such as federated learning and edge cloud learning, which erase discreet elements to reduce decentralized training mechanisms using decentralized data. This approach maintains the patient's anonymity and increases the potential for generalizability.

REFERENCES

[1] Shaikh, Juveriya, Rubeena Khan, Yashwant Ingle, and Nuzhat Shaikh. “Improved skin cancer detection using CNN." International journal of health sciences (Qassim), pp. 14347-14360, 2022.

[2] Mazhar, T.; Haq, I.; Ditta, A.; Mohsan, S.A.H.; Rehman, F.; Zafar, I.; Gansau, J.A.; Goh, L.P.W. “The role of machine learning and deep learning approaches for the detection of skin Cancer”, healthcare, 2023.

[3] Melissa A. Trudrung, Cole Bacig, Brandon Vander Zee, Heather Potter, “Basal cell carcinoma and squamous cell carcinoma of the conjunctiva in a single lesion”, American Journal of Ophthalmology Case Reports, Volume 38, 2025.

[4] Raut, Roshani, Yogini Borole, Sonali Patil, V. N. Khan, and Dattatray G. Takale, “Skin disease classification using machine learning algorithms”, Neuro Quantology 20, no. 10, pp. 9624-9629, 2022.

[5] Balasundaram, A. Shaik, B. R. Alroy, A. Singh and S. J. Shivaprakash, “Genetic Algorithm optimized stacking approach to skin disease detection”, IEEE Access, vol. 12, pp. 88950-88962, 2024.

[6] Srinivasu, P.N.; SivaSai, J.G.; Ijaz, M.F.; Bhoi, A.K.; Kim, W.; Kang, J.J, “Classification of skin disease using deep learning neural networks with Mobile Net V2 and LSTM”, Sensors 2021.

[7] K. Lee et al., “Multi-Task and Few-Shot Learning-Based Fully Automatic Deep Learning Platform for Mobile Diagnosis of Skin Diseases”, IEEE journal of biomedical and health informatics, vol. 27, no. 1, pp. 176-187, 2023.

[8] Rashid, J.; Ishfaq, M.; Ali, G.; Saeed, M.R.; Hussain, M.; Alkhalifah, T.; Alturise, F.; Samand, N, “Skin cancer disease detection using transfer learning technique”, Applied Science, 2022.

[9] M. Fahaad Almufareh, “An Edge computing-based factor-aware novel framework for early detection and classification of melanoma disease through a Customized VGG16 Architecture with privacy preservation and real-time analysis”, IEEE Access, vol. 12, pp. 113580-113596, 2024.

[10] Jagdish, M., Gualán Guamangate, S. P., López, M. A. G., De La Cruz-Vargas, J. A., and Camacho, M. E. R, “Advance study of skin diseases detection using image processing methods”, 2022.

[11] P. Yao et al., "Single Model Deep Learning on Imbalanced Small Datasets for Skin Lesion Classification," in IEEE Transactions on Medical Imaging, vol. 41, no. 5, pp. 1242-1254, 2022.

[12] Gairola, A. K., Kumar, V., Sahoo, A. K., Diwakar, M., Singh, P., and Garg, D, “Multi-feature fusion deep network for skin disease diagnosis”, Multimedia Tools and Applications, 84(1), pp.419-444, 2025.

[13] A. A. Salam, M. Usman Akram, M. Haroon Yousaf and B. Rao, “Derma Trans Net: where transformer attention meets U-Net for skin image segmentation”, IEEE Access, vol. 13, pp. 64305-64329, 2025.

[14] Rokade, Sonali, and Nilamadhab Mishra, “A blockchain-based deep learning system with optimization for skin disease classification”, Biomedical Signal Processing and Control, 2024.

[15] K. Thurnhofer-Hemsi, E. López-Rubio, E. Domínguez and D. A. Elizondo, “Skin Lesion classification by ensembles of deep convolutional networks and regularly spaced shifting”, IEEE Access, vol. 9, pp. 112193-112205, 2021.

[16] Reddy, D. A., Roy, S., Kumar, S., & Tripathi, R, “Enhanced U-Net segmentation with ensemble convolutional neural network for automated skin disease classification”, Knowledge and Information Systems, 65(10), pp. 4111-4156, 2023.

[17] M. Gallazzi, S. Biavaschi, A. Bulgheroni, T. M. Gatti, S. Corchs and I. Gallo, "A large dataset to enhance skin cancer classification with transformer-based deep neural networks”, IEEE Access, vol. 12, pp. 109544-109559, 2024.

[18] Anand, V.; Gupta, S.; Altameem, A.; Nayak, S.R.; Poonia, R.C.; Saudagar, A.K.J. “An Enhanced transfer learning based classification for diagnosis of Skin Cancer”, Diagnostics 2022.

[19] K. Thurnhofer-Hemsi, E. López-Rubio, E. Domínguez and D. A. Elizondo, “Skin Lesion Classification by Ensembles of Deep Convolutional Networks and Regularly Spaced Shifting”, IEEE Access, vol. 9, pp. 112193-112205, 2021.

[20] Gouda, W., Sama, N. U., Al-Waakid, G., Humayun, M., and Jhanjhi, N. Z, “Detection of skin cancer based on skin lesion images using deep learning”, In Healthcare, Vol. 10, no. 7, 2022.

[21] R. Mittal, F. Jeribi, R. J. Martin, V. Malik, S. J. Menachery and J. Singh, "DermCDSM: Clinical decision support model for dermatosis using systematic approaches of machine learning and deep learning," in IEEE Access, vol. 12, pp. 47319-47337, 2024.

[22] Rajeswari, R., P. G. Sivagaminathan, and A. R. Arunachalam, “Skin cancer detection and classification using deep learning techniques”, Deep Learning in Medical Image Analysis. Chapman and Hall/CRC, pp. 97-117, 2024.

[23] Q. Sun, Y. Tang, S. Wang, J. Chen, H. Xu and Y. Ling, “A Deep learning based melanocytic nevi classification algorithm by leveraging physiologic-inspired knowledge and channel encoded information”, IEEE Access, vol. 12, pp. 113072-113086, 2024.

[24] Jain, S.; Singhania, U.; Tripathy, B.; Nasr, E.A.; Aboudaif, M.K.; Kamrani, A.K, “Deep learning-based transfer learning for classification of Skin cancer”, Sensors, 2021.

[25] Ashtagi, R., Kharat, P. V., Sarmalkar, V., Hosmani, S., Patil, A. R., Akkalkot, A. I., and Padthe, A, “Enhancing melanoma skin cancer diagnosis through transfer learning: An EfficientNetb0 approach”, Acadlore Transactions on AI and Machine Learning, 3(1), 57-69, 2024.

[26] Imam, M. H., Nahar, N., Rahman, M. A., and Rabbi, F, “Enhancing skin cancer classification using a fusion of Dense-net and Mobile-net models: a deep learning ensemble approach”, Multidisciplinary Science Journal, 6(7), pp. 2024117-2024117, 2024.

[27] Bello, A.; Ng, S.C., Leung, M.-F, “Skin cancer classification using fine-tuned transfer learning of DENSENET-121”, Applied Science, 2024.

[28] Khan, M. A., Alam, S., and Ahmed, W, “Enhanced skin cancer diagnosis via deep convolutional neural networks with ensemble learning”, SN Computer Science, 6(2), pp. 1-14, 2025.

[29] Natha, P. R. I. Y. A., and P. R. Rajeswari, “Skin cancer detection using machine learning classification models”, International Journal of Intelligent Systems and Applications in Engineering, pp. 139-145, 2024.

[30] Jain, Satin, Udit Singhania, Balakrushna Tripathy, Emad Abouel Nasr, Mohamed K. Aboudaif, and Ali K. Kamrani, “Deep learning-based transfer learning for classification of skin cancer”, Sensors 21, no. 23, 2021.

[31] Huang, Hsin-Wei, et al, “Development of a light-weight deep learning model for cloud applications and remote diagnosis of skin cancers”, The Journal of dermatology, pp. 310-316, 2021.

[32] Chaturvedi, S. S., Tembhurne, J. V., and Diwan, T, “A multi-class skin Cancer classification using deep convolutional neural networks”, Multimedia Tools and Applications, 79(39), pp. 28477-28498, 2020.

[33] Chaturvedi, S. S., Gupta, K., & Prasad, P. S, “Skin lesion analyser: an efficient seven-way multi-class skin cancer classification using MobileNet”, In Advanced machine learning technologies and applications: proceedings of AMLTA, Springer Singapore. pp. 165-176, 2020.